TECHNICAL INFORMATION SERIES

R64SD14

CHEMICALLY REACTING BOUNDARY LAYERS

M. LENARD

SPACE SCIENCES LABORATORY
GENERAL ELECTRIC
MISSILE AND SPACE DIVISION

SPACE SCIENCES LABORATORY

AEROPHYSICS SECTION

CHEMICALLY REACTING BOUNDARY LAYERS

By

M. Lenard

Some parts of this report have been presented at the Eighth Symposium on Ballistic Missile and Space Technology, San Diego, California, October 16-18, 1963

Work performed under Contract No. AF 04(694)-222

R64SD14
March, 1964

MISSILE AND SPACE DIVISION

GENERAL ELECTRIC

CONTENTS

ABSTRACT

Numerical calculations of the chemically reacting laminar air boundary layer equations are presented at several points along cone-shaped reentry bodies at several flight conditions and different wall temperatures. These results use a seven component, ten reaction model of air (N, O, N_2, O_2, NO, NO^+, e^-). Thermodynamic and transport properties are completely general and use the latest available information. The solutions are based on the assumption of local similarity. The resulting electron densities are noted.

INTRODUCTION

Accurate determination of electron densities in the plasma sheath surrounding reentry bodies is important for several reasons. The presence of electrons can interfere with the transmission of signals to and from the vehicle; furthermore, electrons furnish one of the observables present in the wake of reentry bodies. At high altitudes, the effect of finite reaction rates on the amount of ionization can not be neglected.

Calculations of electron densities in the plasma sheath surrounding a reentry vehicle are usually based on an accurate description of the inviscid shock layer surrounding the vehicle. Viscous effects are neglected because they are limited to a thin boundary layer near the surface of the vehicle, which, due to its small size relative to the shock layer thickness, can be neglected as a significant source of electrons. Most of the energy is imparted to the air by means of the shock and pressure forces rather than surface friction or shear forces; this corresponds to a large pressure drag and a comparatively small friction drag for the vehicle, the usual case for blunt reentry bodies. For small tipped slender shapes, the situation is different; much of the energy is imparted to the air by means of surface friction, consequently, the boundary layer will be a very significant (if not the only) source of high temperature air. Therefore, for slender reentry shapes, it is necessary to calculate air boundary layer properties accurately, based on a realistic model of high temperature air which accounts for the principal ionized species. For the flight conditions corresponding to ballistic reentry, it was found that a model including NO^+ as the only ionized species is adequate. In order to account for the possibility of the absence of chemical equilibrium, chemical changes must be accounted for by incorporating the chemical kinetics into the boundary layer equations. A seven component-ten reaction model is the simplest realistic model that can account for the production of NO^+ ions; it forms the basis of this study.

THE BOUNDARY LAYER EQUATIONS

The boundary layer equations for steady axially-symmetric flow of a multi-component reacting mixture have been stated in the literature several times [1, 2]; they are repeated below for reference.

Continuity:

$$\frac{\partial \rho u r}{\partial x} + \frac{\partial \rho v r}{\partial y} = 0 \tag{1}$$

Momentum:

$$\rho u \frac{\partial u}{\partial x} + \rho v \frac{\partial u}{\partial y} + \frac{\partial p}{\partial x} = \frac{\partial}{\partial y} \mu \frac{\partial u}{\partial y} \tag{2}$$

Energy:

$$\left[\rho u \frac{\partial T}{\partial x} + \rho v \frac{\partial T}{\partial y}\right] \sum_{i=1}^{n} c_i \frac{dh_i}{dT} - u \frac{dp}{dx} = \frac{\partial}{\partial y} k \frac{\partial T}{\partial y} + \mu \left(\frac{\partial u}{\partial y}\right)^2$$

$$- \rho \frac{\partial T}{\partial y} \sum_{i=1}^{n} q_i c_i \frac{dh_i}{dT} - \sum_{i=1}^{n} w_i h_i \tag{3}$$

Species Conservation:

$$\rho u \frac{\partial c_i}{\partial x} + \rho v \frac{\partial c_i}{\partial y} + \frac{\partial}{\partial y} (\rho c_i q_i) = w_i \tag{4}$$

These are the principal differential equations. Additional differential equations are needed to relate the diffusional flux velocities of the species across the boundary layer, q_i, to the concentration gradients. Two alternate formulations are given by Hirschfelder, Curtiss and Bird [3] as follows:

$$\sum_{\substack{j=1 \\ j \neq i}}^{n} \frac{M^2}{m_j} \frac{c_i c_j}{\mathcal{D}_{ij}} (q_j - q_i) = \frac{\partial}{\partial y} M c_i \tag{5}$$

or, alternately;

$$c_i q_i = \sum_{j=1}^{n} \frac{m_i}{M^2} D_{ij} \frac{\partial}{\partial y} Mc_j \qquad (6)$$

where the binary diffusion coefficients $\mathcal{D}_{ij}$ in Eq. (5) are functions of temperature only, but the mixture diffusion coefficients D_{ij} in Eq. (6) depend both on temperature and local concentrations and are actually calculated by solving the system of n - 1 independent Eqs. (5) for the q_i - s. The formulation of the flux velocities of ionized species in a neutral mixture is somewhat different from the above and will be subsequently discussed.

In addition to the above system of differential equations, which can be thought of as representing equations for the principal variables v, u, T and the n - 1 independent c_i - s, additional equations are available that relate the thermodynamic properties, transport properties, and composition of the mixture to each other; e.g.:

Equation of State:

$$\frac{p}{R} = \frac{\rho T}{M} = \text{constant} \qquad (7)$$

Mixture Molecular Weight:

$$\frac{1}{M} = \sum_{i=1}^{n} \frac{c_i}{m_i} \qquad (8)$$

Mass Concentrations:

$$\sum_{i=1}^{n} c_i = 1 \qquad (9)$$

Species Enthalpies:

$$h_i = h_i(T) \qquad (10)$$

The dependence of species enthalpies on temperature is based on Langelo's[4] work.

Chemical Mass Generation Rates:

$$w_i = w_i (\rho, T, c_j) \tag{11}$$

are based on Bortner's[5] recent survey report.

Transport properties of the mixture are calculated by means of Wilke's semi-empirical formula [e.g. Reference 6]. The temperature dependence of the species viscosities and binary diffusion coefficients is based on unpublished work by Baulknight[7] and on results published by Yun, Weissman, and Mason[8, 9]. For the details of the kinetic system, thermodynamic and transport properties, the reader is referred to Appendices 1 through 3.

The diffusion coefficients for electrons need not be calculated separately, because under all conditions of practical interest the Debye shielding length in the ionized air will be so small that the gas will be electrically neutral at every point, implying simultaneous diffusion of ions and electrons. This simultaneous diffusion of the combined ion-electron species can be calculated by a method suggested by K. T. Yen and confirmed by C. Curtiss, as follows. Let there be a separation between the ions and electrons on a microscopic scale, so that a local electric field is created in the flowing ionized gas. For the ions and electrons, Eq. (5) is then modified to include the effect of an electrostatic body force caused by this local microscopic electric field:

$$\sum_{\substack{j=1 \\ j \neq NO^+}}^{n} \frac{M^2}{m_j m_{NO^+}} \frac{c_{NO^+} c_j}{\mathcal{D}_{NO^+ j}} (q_j - q_{NO^+}) = \frac{\partial}{\partial y} M \frac{c_{NO^+}}{m_{NO^+}} - \mathcal{E} \frac{c_{NO^+}}{m_{NO^+}} \tag{12}$$

$$\sum_{\substack{j=1 \\ j \neq e^-}}^{n} \frac{M^2}{m_j m_{e^-}} \frac{c_{e^-} c_j}{\mathcal{D}_{e^- j}} (q_j - q_{e^-}) = \frac{\partial}{\partial y} M \frac{c_{e^-}}{m_{e^-}} + \mathcal{E} \frac{c_{e^-}}{m_{e^-}}$$

where the body force $\mathcal{E}$ has the same magnitude but the opposite sign for the ions and electrons. Since in a neutral plasma

$$q_{e^-} = q_{NO^+}$$

$$\frac{c_{e^-}}{m_{e^-}} = \frac{c_{NO^+}}{m_{NO^+}} \tag{13}$$

Eqs. (12) can be added to eliminate the body force term;

$$\sum_{\substack{j=1 \\ j \neq NO^+}}^{n} \frac{M^2}{m_j} c_{NO^+} + c_j (q_j - q_{NO^+}) \left[\frac{1}{\mathcal{D}_{NO^+ j}} + \frac{1}{\mathcal{D}_{e^- j}} \right] = 2 \frac{\partial}{\partial y} Mc_{NO^+} \tag{14}$$

where this equation describes the diffusion of the combined $NO^+ - e^-$ ion-electron species in the mixture. The additional assertion can now be made that the mobility of the electrons is much larger than that of the ions or neutrals, so that

$$\mathcal{D}_{e^- j} >> \mathcal{D}_{ij} \tag{15}$$

for all i and j. Terms of the order $\mathcal{D}_{ij}/\mathcal{D}_{e^- j}$ can then be neglected in the equations so that the final expressions for the interdiffusion of the various neutral species and the combined ion-electron species become;

$$\sum_{\substack{j=1 \\ j \neq i, e^-}}^{n} \frac{M^2}{m_j} \frac{c_i c_j}{\mathcal{D}_{ij}} (q_j - q_i) = \frac{\partial}{\partial y} Mc_i \quad \text{for } i \neq NO^+$$

$$\sum_{\substack{j=1 \\ j \neq NO^+, e^-}}^{n} \frac{M^2}{m_j} \frac{c_{NO^+} c_j}{\mathcal{D}_{NO^+ j}} (q_j - q_{NO^+}) = 2 \frac{\partial}{\partial y} Mc_{NO^+} \tag{16}$$

which is a generalization of the ambipolar diffusion in a neutral-ion-electron mixture. Eqs. (16) replace (5); correspondingly, Eq. (6) is modified by solving for the n - 2 independent q_i - s from Eq. (16).

BOUNDARY CONDITIONS

Eqs. (1) through (4), (7) through (11), and (16) represent the system of equations that have to be solved for the seven component model of air under consideration. Boundary conditions for the equations are furnished by specifying conditions at the wall and in the external (inviscid) flow.

At the wall (y = 0);

$$u(x, 0) = v(x, 0) = 0$$
$$T(x, o) = T_w(x) \tag{17}$$

In addition to Eq. (17), boundary conditions on concentrations c_i must also be stated at the wall. At a wall where there is no mass injection two types of boundary conditions are usually considered. On a wall that is not catalytic, there are no surface reactions, therefore there can be no flux of species to and from the wall. Thus,

$$q_i(x, 0) = 0 \tag{18}$$

for all i, which implies that

$$\left.\frac{\partial c_i}{\partial y}\right|_{y=0} = 0 \tag{19}$$

at y = 0. A catalytic wall can cause sudden changes in composition due to surface reactions; usually the assumption is made that the mixture is at chemical equilibrium at the local (wall) temperature. This can be denoted by:

$$c_i(x, 0) = c_{i\,eq}(T_w, p, c^j) \tag{20}$$

where the above expression indicates that in order to determine the chemical equilibrium concentrations of the various species, it is necessary to know in addition to temperature and pressure the mass fractions of the chemical elements (denoted by superscript j) that comprise the reacting mixture. Due to the interdiffusion of the various species, the mass fraction of the various elements in the boundary layers cannot be known a priori, not even if instantaneous local chemical equilibrium can be assumed everywhere. In order to show this, one may relate the mass fraction of the j-th element in the mixture to the mass fractions of the n species by

$$c^j = \sum_{i=1}^{n} \frac{m^j}{m_i} \alpha_i^j c_i \tag{21}$$

where α_i^j is the number of atoms of element j in the i-th species, and the m are the respective molecular (or atomic) weights. Since elements are conserved in a chemical reaction, i.e.:

$$\sum_{i=1}^{n} \frac{m^j}{m_i} \alpha_i^j w_i = 0 \tag{22}$$

an equation for the conservation of elements can be written by utilizing Eqs. (20), (21), in conjunction with Eq. (4);

$$\rho u \frac{\partial c^j}{\partial x} + \rho v \frac{\partial c^j}{\partial y} + \frac{\partial}{\partial y} \left(\rho \sum_{i=1}^{n} \frac{m^j}{m_i} \alpha_i^j c_i q_i \right) = 0 \tag{23}$$

Eq. (23) above indicates that in general, the mass fraction of the elements in the boundary layer will change irrespective of what the reaction rates are. In particular then, the mass fraction of the elements will not be known at the wall, which implies that additional information is necessary to define the boundary conditions for species concentrations at a catalytic wall. If the n species are made up of m elements, then there will be only n - m independent boundary conditions of the type shown in Eq. (20) (one less if e^- is one of the species and a neutral plasma is specified). To obtain the m - 1 additional boundary conditions necessary at the wall, the conservation of elements in the surface reactions that are implied by the catalytic wall must be stated;

$$\sum_{i=1}^{n} \frac{m^j}{m_i} \alpha_i^j q_i(x, 0) c_i(x, 0) = 0 \tag{24}$$

where there are m - 1 independent boundary conditions of the type shown in Eq. (24), corresponding to the m - 1 independent elemental concentrations. For the present seven component mixture, over-all mass conservation (Eq. 9) and charge conservation leave essentially five independent species conservation Eq. (4) to be considered. The mixture contains two elements, O and N, the concentration of one of which is independent. Thus, there will be four boundary conditions of the type shown in Eq. (20) available; the four species must include at least, but not more than, one charged species and at least one species which is comprised of pure N and pure O

each. In addition, one boundary condition of the type shown in Eq. (24) is available to relate the slopes of the concentration profiles at the wall.

Far from the wall the boundary layer solution must merge into the external inviscid flow, which is specified. This implies that as

$$\begin{aligned} y &\to \infty \\ u &\to u_e \\ T &\to T_e \\ c_i &\to c_{ie} \end{aligned} \tag{25}$$

Corresponding to the seven boundary conditions shown in (25) there will be seven unknown boundary values of the appropriate variables at the wall, which can be determined only by solving the boundary layer equations. In a numerical computation scheme, an iteration on these seven unknowns has to be performed in order to integrate the equations and obtain the proper solutions that satisfy boundary conditions (25). Two of the seven unknown boundary values are;

$$\left.\frac{\partial u}{\partial y}\right|_{y=0} \qquad \left.\frac{\partial T}{\partial y}\right|_{y=0} \tag{26}$$

For a wall that is not catalytic, the additional unknown boundary values are;

$$c_i(x, 0) \tag{27}$$

which corresponds to Eq. (18) and (19). For a catalytic wall, the unknown quantities are;

$$c^N(x, 0) \text{ or } c^O(x, 0) \qquad q_i(x, 0) \tag{28}$$

where the four species i in Eq. (28) correspond to the four species for which boundary conditions are specified by Eq. (20).

TRANSFORMATION OF THE EQUATIONS

Solution of the foregoing system of partial differential equations can be greatly simplified if the independent variables are transformed in accordance with the combined Mangler and Howarth-Dorodnytsin transformations (cf. References 1, 2, 10):

$$\xi = \int_o^x \rho_w \mu_w u_e r^2 \, dx \qquad (29)$$

$$\eta = \frac{u_e r}{\sqrt{2\xi}} \int_o^y \rho \, dy .$$

If, in addition, the velocity is expressed as

$$u = u_e \frac{\partial f}{\partial \eta} \qquad (30)$$

the continuity Eq. (1) can be used to express v in terms of f, and the remaining differential equations can be written in terms of the new variables η and ξ. The present development is essentially the same as that of Fay and Riddell [1] except for the more exact formulation of the species flux velocities [Eqs. (16), (5) and (6)]. The final form of the transformed boundary layer equations becomes:

Momentum:

$$\frac{\partial}{\partial \eta}\left(\ell \frac{\partial^2 f}{\partial \eta^2}\right) + f \frac{\partial^2 f}{\partial \eta^2} + \beta\left[\frac{\rho_e}{\rho} - \left(\frac{\partial f}{\partial \eta}\right)^2\right] = 2\xi\left[\frac{\partial f}{\partial \eta}\frac{\partial^2 f}{\partial \eta \partial \xi} - \frac{\partial f}{\partial \xi}\frac{\partial^2 f}{\partial \eta^2}\right] \qquad (31)$$

Energy:

$$\frac{\partial}{\partial \eta}\left[\frac{\ell}{Pr}\sum_{i=1}^{7} c_i \frac{dh_i}{dT}\left(\frac{T_e}{h_e}\right)\frac{\partial}{\partial \eta}\left(\frac{T}{T_e}\right)\right] + f\sum_{i=1}^{7} c_i \frac{\partial}{\partial \eta}\left(\frac{h_i}{h_e}\right) -$$

$$-\sum_{i=1}^{7} \frac{\beta w_i}{\rho \frac{du_e}{dx}}\left(\frac{h_i}{h_e} + \frac{u_e^2}{h_e}\right)\left\{\ell\left(\frac{\partial^2 f}{\partial \eta^2}\right)^2 + \right.$$

$$+ \beta \frac{\partial f}{\partial \eta} \left[\frac{T}{T_e} \left(\frac{\sum_{i=1}^{7} c_i \frac{dh_i}{dT}}{\sum_{i=1}^{7} c_{ie} \frac{dh_{ie}}{dT}} + \frac{2h_e}{\beta u_e^2} \sum_{i=1}^{7} \frac{\partial c_{ie}}{\partial \ln \xi} \frac{h_{ie}}{h_e} \right) - \frac{\rho_e}{\rho} \right] \Bigg\} -$$

(32)

$$- \frac{\rho^2}{h_e \rho_w \mu_w} \frac{\partial T}{\partial \eta} \sum_{i=1}^{7} \frac{q_i}{\eta_y} c_i \frac{dh_i}{dT} = 2\xi \sum_{i=1}^{7} c_i \left\{ \frac{\partial f}{\partial \eta} \frac{\partial}{\partial \xi} \left(\frac{h_i}{h_e} \right) - \right.$$

$$\left. - \frac{\partial f}{\partial \xi} \frac{\partial}{\partial \eta} \left(\frac{h_i}{h_e} \right) \right\}$$

where

$$Pr \equiv \frac{\mu}{k} \sum_{i=1}^{7} c_i \frac{dh_i}{dT} \equiv \frac{hc_p}{k} \tag{33}$$

$$\ell \equiv \frac{\rho \mu}{\rho_w \mu_w}$$

$$\beta \equiv \frac{2\xi}{u_e} \frac{du_e}{d\xi} = \frac{2\xi}{\rho_w \mu_w u_e^2 r^2} \frac{du_e}{dx}$$

and where the flux velocities are determined from a transformation of Eqs. (16);

$$\sum_{\substack{i=1 \\ j \neq i, e^-}}^{n} \frac{M^2}{m_j} \frac{c_i c_j}{\mathcal{D}_{ij}} \frac{q_i - q_j}{\eta_y} = \frac{\partial}{\partial \eta} M c_i \text{ for } i \neq NO^+$$

(34)

$$\sum_{\substack{j=1 \\ j \neq NO^+, e^-}}^{n} \frac{M^2}{m_j} \frac{c_{NO^+} c_j}{\mathcal{D}_{NO^+ j}} \frac{q_j - q_{NO^+}}{\eta_y} = 2 \frac{\partial}{\partial \eta} M c_{NO^+}$$

Noting first that in accordance with transformations (29);

$$\frac{1}{\eta_y}\frac{\partial}{\partial\eta}\eta_y f(\eta) = \frac{1}{\rho}\frac{\partial}{\partial\eta}\rho f(\eta)$$

for any function $f(\eta)$ of η, the species conservation equations can finally be written;

$$f\frac{\partial c_i}{\partial\eta} - \frac{1}{\rho_w\mu_w}\frac{\partial}{\partial\eta}\left(\rho^2 c_i\frac{q_i}{\eta_y}\right) + \frac{\beta}{\frac{du_e}{dx}}\left[\frac{w_i}{\rho} - f_\eta\frac{c_i}{c_{ie}}\left(\frac{w_i}{\rho}\right)_e\right]$$

$$= 2\xi\left[\frac{\partial f}{\partial\eta}\frac{\partial c_i}{\partial\xi} - \frac{\partial f}{\partial\xi}\frac{\partial c_i}{\partial\eta} - \frac{\partial f}{\partial\eta}\frac{c_i}{c_{ie}}\frac{\partial c_{ie}}{\partial\xi}\right] \tag{35}$$

Auxiliary Eqs. (7) through (11) are not affected by the transformations; the boundary conditions are likewise unaffected, except for the velocities at the wall, instead of Eq. (17) the boundary conditions are:

$$f(\xi 0) = \left.\frac{\partial f}{\partial\eta}\right|_{\eta=0} = 0 \tag{36}$$

$$T(\xi 0) = T_w(\xi)$$

The boundary conditions at the wall for the concentrations are unchanged from those specified by either Eq. (19) (non-catalytic surface) or Eqs. (20) and (24) (catalytic surface). Far from the wall, boundary conditions shown in Eq. (25) are equivalent to

$$\eta \to \infty$$

$$\frac{\partial f}{\partial\eta} \to 1 \tag{37}$$

$$T(\xi,\eta) \to T_e(\xi)$$

$$c_i(\xi,\eta) \to c_{ie}(\xi)$$

The terms that appear on the right hand sides of the foregoing system of seven simultaneous differential equations are the so called "non-similar" terms. At the stagnation point these non-similar terms vanish and the partial differential equations simplify to ordinary ones. Fay and Ridell [1] have pointed out that these terms can sometimes be neglected as an approximation based on physical considerations other than the rigorously justifiable

stagnation point case. (Note that in the above formulation these non-similar terms are always zero at the wall and far from the wall.) Neglecting the non-similar terms results in the so called "locally similar" solutions, which can always be justified a posteriori, provided the profile shapes change slowly. The results described in this report are based on this assumption of local similarity.

NUMERICAL RESULTS

Numerical solutions of the foregoing system of boundary layer equations have been obtained. The method of solution makes the assumption of local similarity and computes the results at a certain specified point along the body. To solve the resulting system of seven ordinary differential equations, seven unknown boundary conditions at the wall are assumed and a numerical integration performed to the edge of the boundary layer. There the results are compared with the seven required boundary conditions, and then an iteration procedure performed on the seven assumed wall boundary conditions, repeating the integration a sufficient number of times to reach agreement with the edge boundary conditions to the required accuracy. (This type of procedure is described in detail in Appendix B of Reference 11.)

The results of these calculations, which are all based on a fully catalytic wall assumption, are shown in Figs. 1 through 9 and Table 1. The principal example that was considered was that of a 10° half angle pointed cone at 22,000 fps speed and 150,000 ft. altitude. Ramifications of possible boundary layer-inviscid flow interactions were not considered; the inviscid flow was assumed to be at chemical equilibrium. (Due to the low temperatures the thermo-chemical model assumed for the inviscid flow is immaterial.) The surface speed, pressure and temperature are 21,590 fps, .02756 atm., and 1061°K respectively. The wall temperature was assumed to be 1000°K.

Comparison of these non-equilibrium results was made to the corresponding equilibrium solution. The latter, while based on simplified fluid properties, still indicates the extent of relaxation toward equilibrium that has taken place. Also, Blottner's[12] recent results furnish a comparison between the exact "non-similar" solution of the partial differential equations and the present results based on the assumption of local similarity.

The variation of temperature in the boundary layer is shown in Fig. 1. These profiles are substantially the same from the tip to 4.5 ft. downstream from the tip. This is in contrast with the profile based on chemical equilibrium where the peak temperatures have been greatly reduced. This indicates that for the conditions that were considered it would take a distance much longer than 4.5 ft. to approach chemical equilibrium in the boundary layer. Figures 2 through 5 show composition profiles for the species O, N, NO and the electron densities respectively. Atomic oxygen is the principal new species in the boundary layer due to the relative ease of oxygen dissociation. Atomic nitrogen

is a comparatively minor species but it is important because of its role in the generation of nitric oxide ions and electrons. (See Appendix 1.) Figure 3 clearly indicates that there is an "overshoot" in the concentration of this important species as compared to the equilibrium value. The reason for this is the higher temperature in the non-equilibrium boundary layer as compared to the equilibrium case, and the comparative ease with which the so called "shuffle" reactions are able to produce nitrogen atoms, provided sufficient amounts of atomic oxygen and nitric oxide are present. Such "overshoot" phenomena have been observed in the relaxation processes behind hypersonic shocks in inviscid flow; they arise from the non-linearities of coupled fluid mechanic and complicated chemical kinetic systems. No such "overshoot" phenomena are exhibited by the nitric oxide concentrations (Fig. 4) and the electron densities (Fig. 5) in the boundary layer. However, the possibility of an electron density "overshoot" occurring for longer bodies or at different flight conditions cannot be ruled out, particularly because such excess electron densities have been predicted behind shocks in inviscid flow (Reference 13). This is significant because it indicates that under some circumstances the electron densities in the non-equilibrium boundary layer can exceed the corresponding equilibrium values.

Fig. 5 also shows an electron density profile calculated by an approximation which appears reasonable; the two-body nitric oxide ionizing reaction was assumed to be at instantaneous equilibrium in conjunction with the locally similar chemical non-equilibrium solution. The resulting prediction was three orders of magnitude too large, indicating that care must be exercised when attempting to simplify complicated chemistry in this problem. (This is in contrast with heat transfer rate calculations where the simplifications of separate decoupled oxygen and nitrogen dissociation reactions, or even the binary atom-molecule fluid assumption have resulted in adequate predictions).

Further insight into the complexities of the reacting air boundary layer can be gained from Figs. 6 through 8. Due to the complex transport properties which govern the interdiffusion of the various reacting species, there will be a variation in the total oxygen content of the boundary layer, as shown in Fig. 6. Fig. 7 shows that the production of electrons occurs mainly in the narrow high temperature region near the wall from where diffusion towards the wall and free stream take place. The sensitivity of the resulting electron densities to the ionizing rate constants and the ambipolar diffusivities is shown in Fig. 8 where the effect of a 1.5-fold increase in ionizing rates and a halving of the ambipolar diffusivities is demonstrated. Figure 9 shows the variation of peak electron densities in the boundary layer along the cone. The locally similar solution predicts a somewhat more rapid adjustment toward equilibrium than the corresponding exact non-similar solution of Reference 12.

Table I shows the effects of changing wall temperature and altitude for this problem as it affects the principal properties of the resulting non-equilibrium air boundary layer. As expected, a rise in wall temperature

increases the chemical activity in the boundary layer whereas an increased altitude diminishes it greatly. Also shown is the effect os simplifying the inter-diffusion of the reacting species by using a constant Lewis number of 1.4 instead of the general multicomponent diffusion coefficients (i.e. $\delta_{ij} = 1.4\ k/\rho c_p$). Finally, a comparison with the non-similar results of Reference 12 is also included.

At the time of writing this report it has become apparent that the numerical procedure used for the locally similar approximation in this report is both less exact and less economical than the procedure described in Reference 12 which calculates non-similar solutions of the same problem.

ACKNOWLEDGMENTS

The numerical results presented here are partly due to the efforts of Dr. James Jewell who designed the computer program, and particularly to the efforts of Mr. Edward Meyer of CEIR Inc. who did the programming and performed the actual computations, thereby furnishing the key ingredient to obtain these numerically difficult results.

Chemical, transport, and thermodynamic properties used in these computations were scrutinized by Dr. H. Li, and assembled by Mr. A. E. Reed.

The use of as yet unpublished results of Dr. F. G. Blottner in this report is gratefully acknowledged.

Table 1. Locally Similar Boundary Layer Properties on 10^{o} Cone at 22,000 fps, 4.5 ft. Downstream from Tip

Method Diffusion Coefficients Altitude, ft.	Non-Similar[12] General 150,000	Locally Similar General 150,000	Locally Similar General 150,000	Locally Similar General 200,000	Locally Similar $\delta_{ij} = 1.4\, k/\rho c_p$ 150,000
P_e, atmospheres	0.02756	0.02756	0.02756	0.0046706	0.02756
U_e, fps	21,590	21,590	21,590	21,590	21,590
T_e, ^{o}K	1061	1061	1061	1041.5	1061
T_w, ^{o}K	1000	1000	1050	1000	1000
T_{max} ^{o}K	4607	4580	4604	4570	4582
$C_{O_{max}}$	1.71×10^{-3}	1.88×10^{-3}	2.00×10^{-3}	0.328×10^{-3}	2.05×10^{-3}
$C_{N_{max}}$	3.01×10^{-6}	3.18×10^{-6}	3.52×10^{-6}	0.378×10^{-6}	3.55×10^{-6}
$C_{NO_{max}}$	2.52×10^{-4}	3.52×10^{-4}	4.02×10^{-4}	0.549×10^{-4}	3.11×10^{-4}
$N_{e^-}{}_{max}$, e^-/cc	4.73×10^{5}	7.74×10^{5}	9.30×10^{5}	0.510×10^{3}	8.03×10^{5}

NOMENCLATURE

c_i	Mass fraction of i-ith species
c^i	Mass fraction of i-th element
c_p	Mixture (frozen) specific heat (Equation 33)
D_{ij}	Mixture diffusion coefficient
$\mathcal{D}_{ij}$	Binary diffusion coefficient
$\mathcal{E}$	Body force due to microscopic electric field
f	Non-dimensional stream function (Equation 30)
h	Mixture enthalpy
h_i	Species enthalpy
k	Mixture (frozen) heat conductivity
ℓ	Density-viscosity product (Equation 33)
Le	Lewis number
m	Number of reactions in chemical system
m_i	Molecular weight of i-th species
M	Molecular weight of mixture
n	Number of species in mixture
p	Pressure
Pr	(Frozen) Prandtl number (Equation 33)
q_i	Diffusional flux velocity of i-th species
r	Radial coordinate of axi-symmetric surface
R	Universal gas constant
T	Absolute temperature

u, v	Parallel and normal velocities in boundary layer
w_i	Chemical mass generate rate of i-th species
x, y	Parallel and normal coordinates in boundary layer
α_i^j	Number of atoms of element j in species i
β	Pressure gradient parameter (Equation 33)
ξ, η	Transformed parallel and normal coordinates in boundary layer (Equation 29)
μ	Viscosity
ρ	Density

SUBSCRIPTS

e	At the outer edge of the boundary layer
eq	In chemical equilibrium
i, j, O	Refers to species (i=th, j-th, O, etc.)
W	Wall

SUPERSCRIPT

i, j, O	Refers to element (i-th, j-th, O, etc.)

REFERENCES

1. Fay, J. A., and Riddell, F. R., "Theory of Stagnation Point Heat Transfer In Dissociated Air", Journal of the Aero/Space Sciences, vol. 25, February 1958.

2. Scala, S. M., and Baulknight, C. W., "Transport and Thermodynamic Properties In a Hypersonic Laminar Boundary Layer, Part 2 Applications", ARS Journal, vol. 30, no. 4, 1960, 329.

3. Hirschfelder, J. O., Curtiss, C. F., and Bird, R. B., Molecular Theory of Gases and Liquids, John Wiley and Sons, 1954.

4. Langelo, V. A., "Inviscid Reacting Flow Field about Hypersonic Bodies", G.E. MSD Space Sciences Laboratory TIS R63SD90 November 1963.

5. Bortner, M. H., "Chemical Kinetics in a Reentry Flow Field", G.E. TIS, MSD Space Sciences Laboratory R63SD63, August 1963.

6. Bird, R. B., Stewart, W. E., Lightfoot, E. N., Transport Phenomena, John Wiley & Sons, 1960.

7. Baulknight, C. W., "Binary Diffusion Coefficients for NO^+", G.E. MSD internal communication, unpublished.

8. Yun, K. S., and Mason, E. A., "Collision Integrals for the Transport Properties of Dissociating Air at High Temperatures", Physics of Fluids, vol. 5, no. 4, 1962, p. 380.

9. Yun, K. S. Weissman, S., and Mason, E. A., "High Temperature Transport Properties of Dissociating Nitrogen and Dissociating Oxygen", Physics of Fluids vol. 5, no. 6, 1962, p. 672.

10. Lees, Lester, "Laminar Heat Transfer Over Blunt-Nosed Bodies at Hypersonic Flight Speeds", Jet Propulsion, vol. 26, 1956.

11. Reshotko, E., and Beckwith, I. E., "Compressible Laminar Boundary Layer Over a Yawed Infinite Cylinder with Heat Transfer and Arbitrary Prandtl Number", NACA Rept. 1379, 1958.

12. Blottner, F. G., "Non-Equilibrium Laminar Boundary Layer Flow of Ionized Air." AIAA Aerospace Sciences Meeting January 1964 Preprint 64-41, also G.E. TIS, to be published.

13. Langelo, V. A., "Chemical Non-Equilibrium Shock Flow", G.E. TIS R63SD66, August 1963.

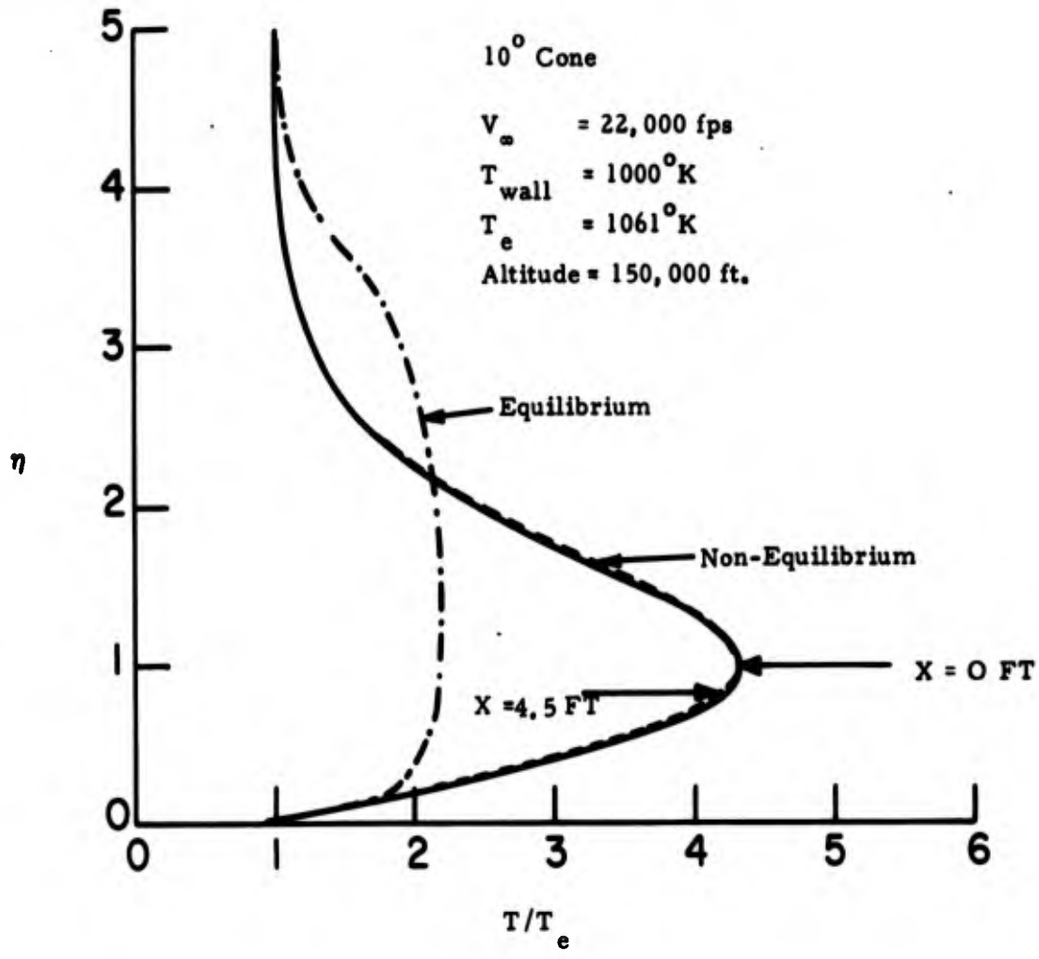

Figure 1. Temperature Profiles for the Non-Equilibrium Boundary Layer Flow for a 10° Cone

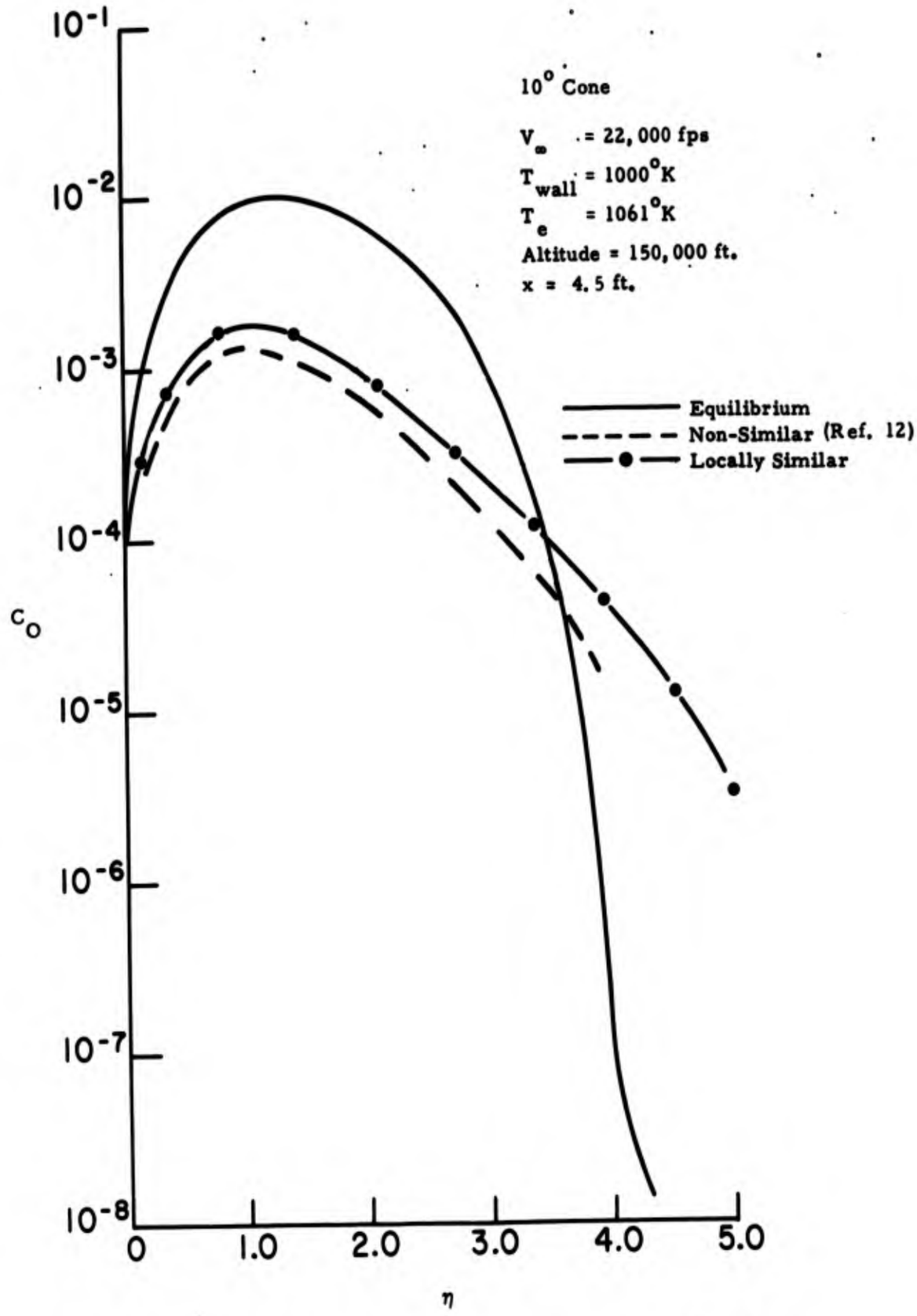

Figure 2. Mass Fraction of Atomic Oxygen Across the Boundary Layer on a 10° Cone

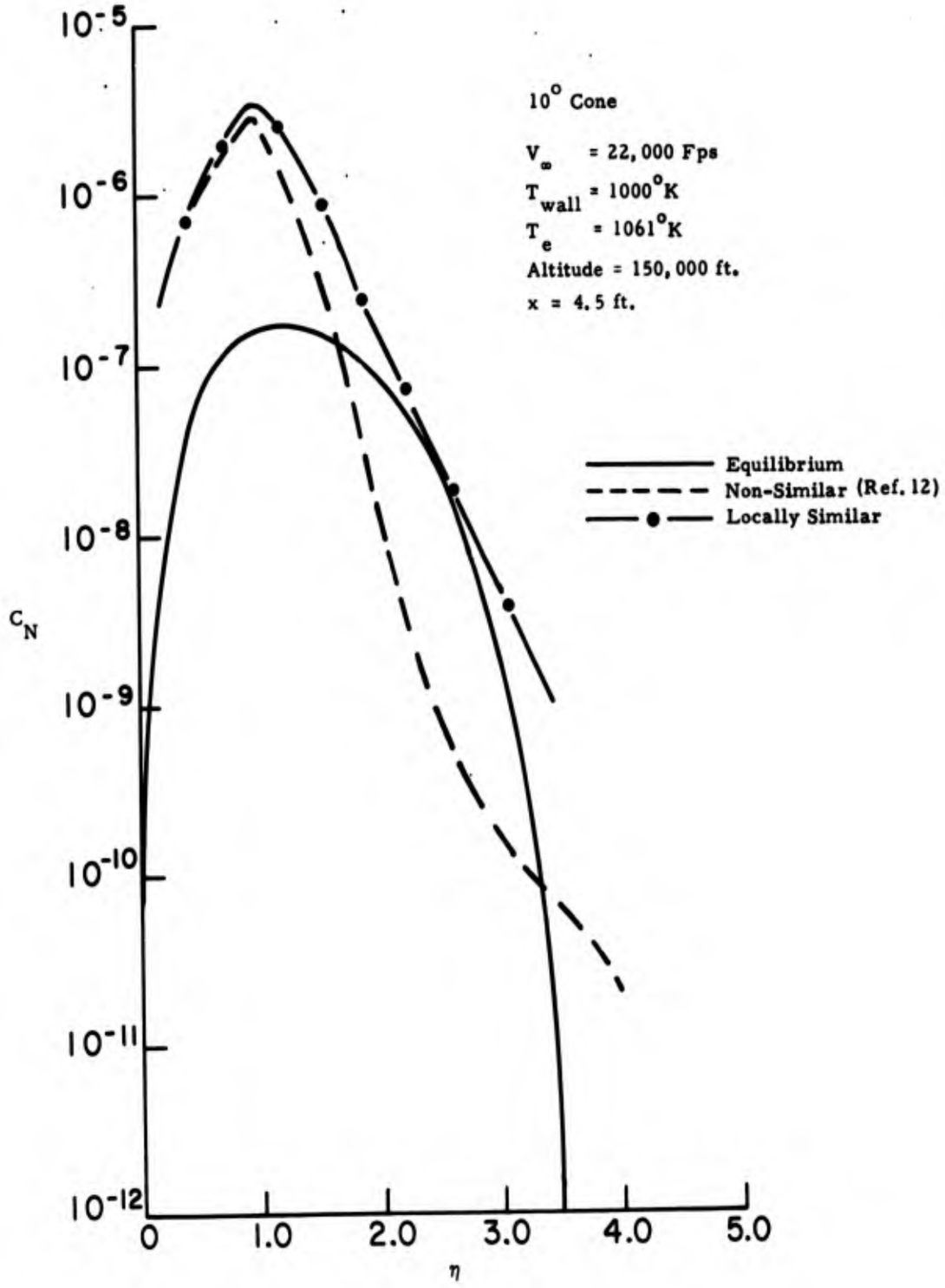

Figure 3. Mass Fraction of Atomic Nitrogen Across the Boundary Layer on a 10° Cone

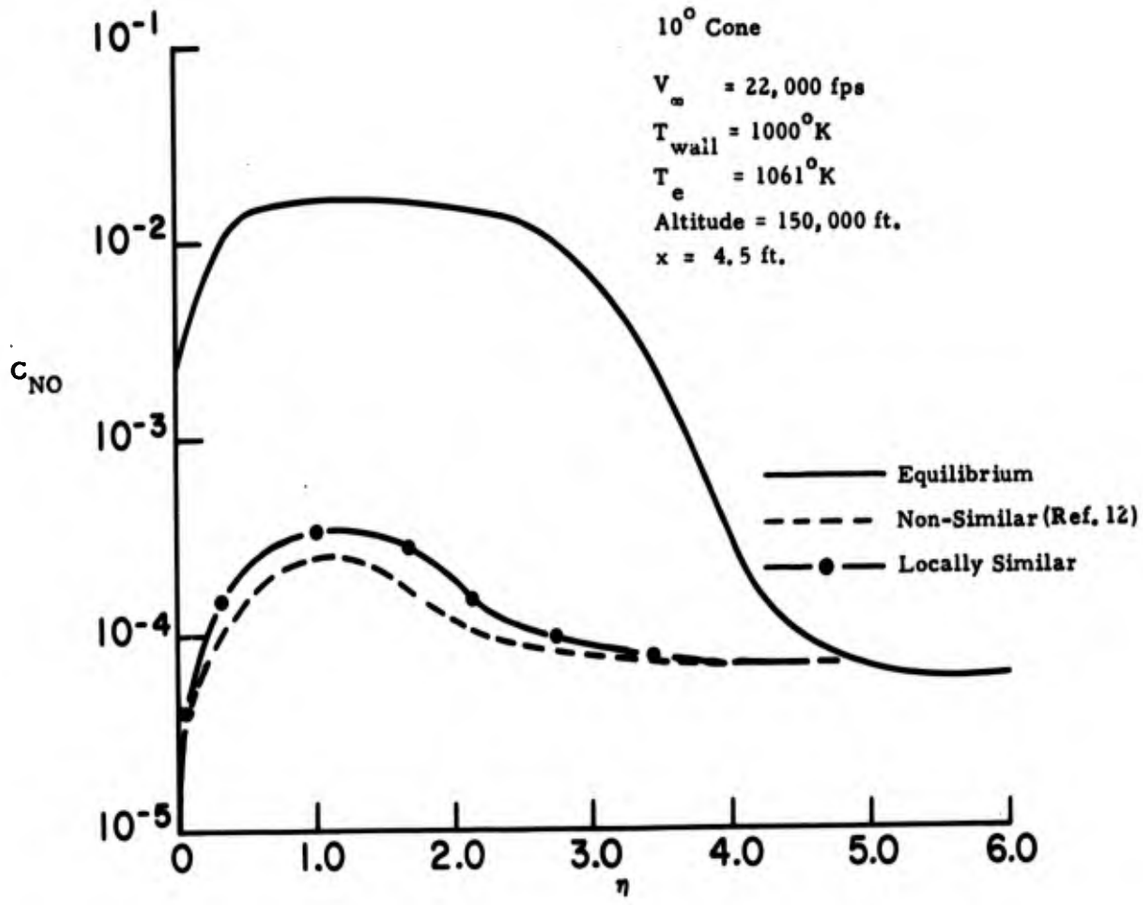

Figure 4. Mass Fraction of Nitric Oxide Across the Boundary Layer on a 10° Cone

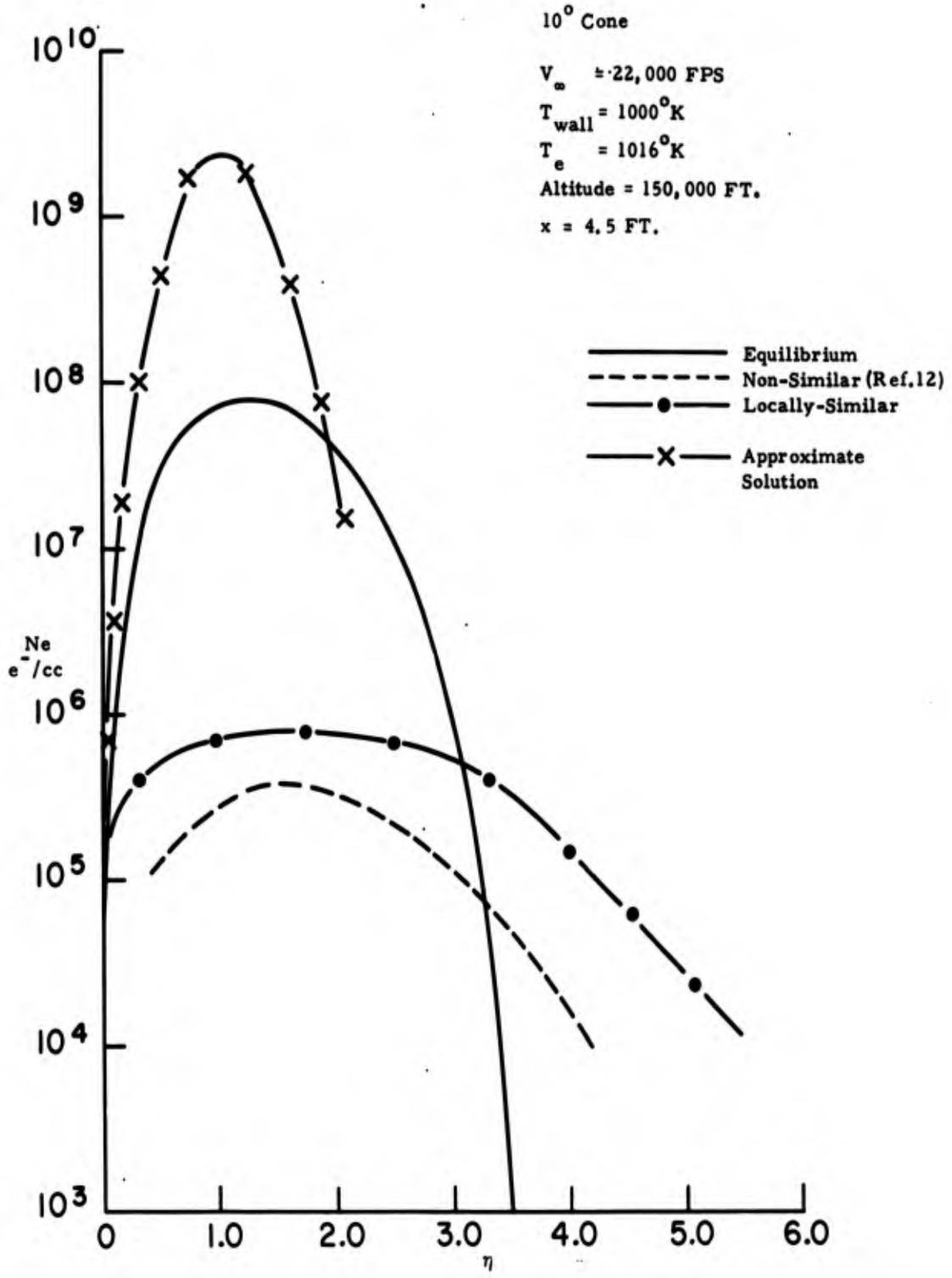

Figure 5. Electron Density in the Boundary Layer on a 10° Cone

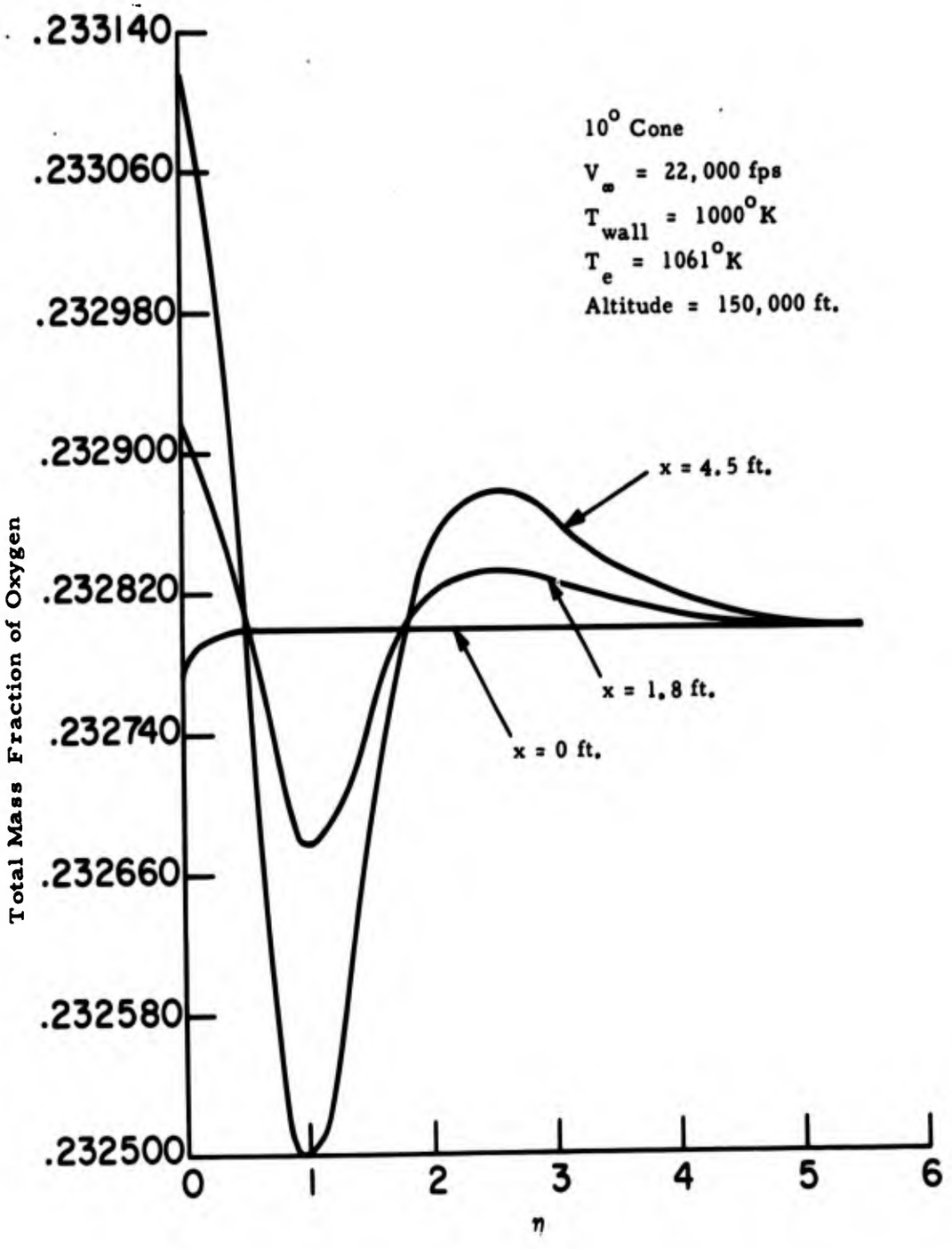

Figure 6. Total Oxygen Content in Boundary Layer.

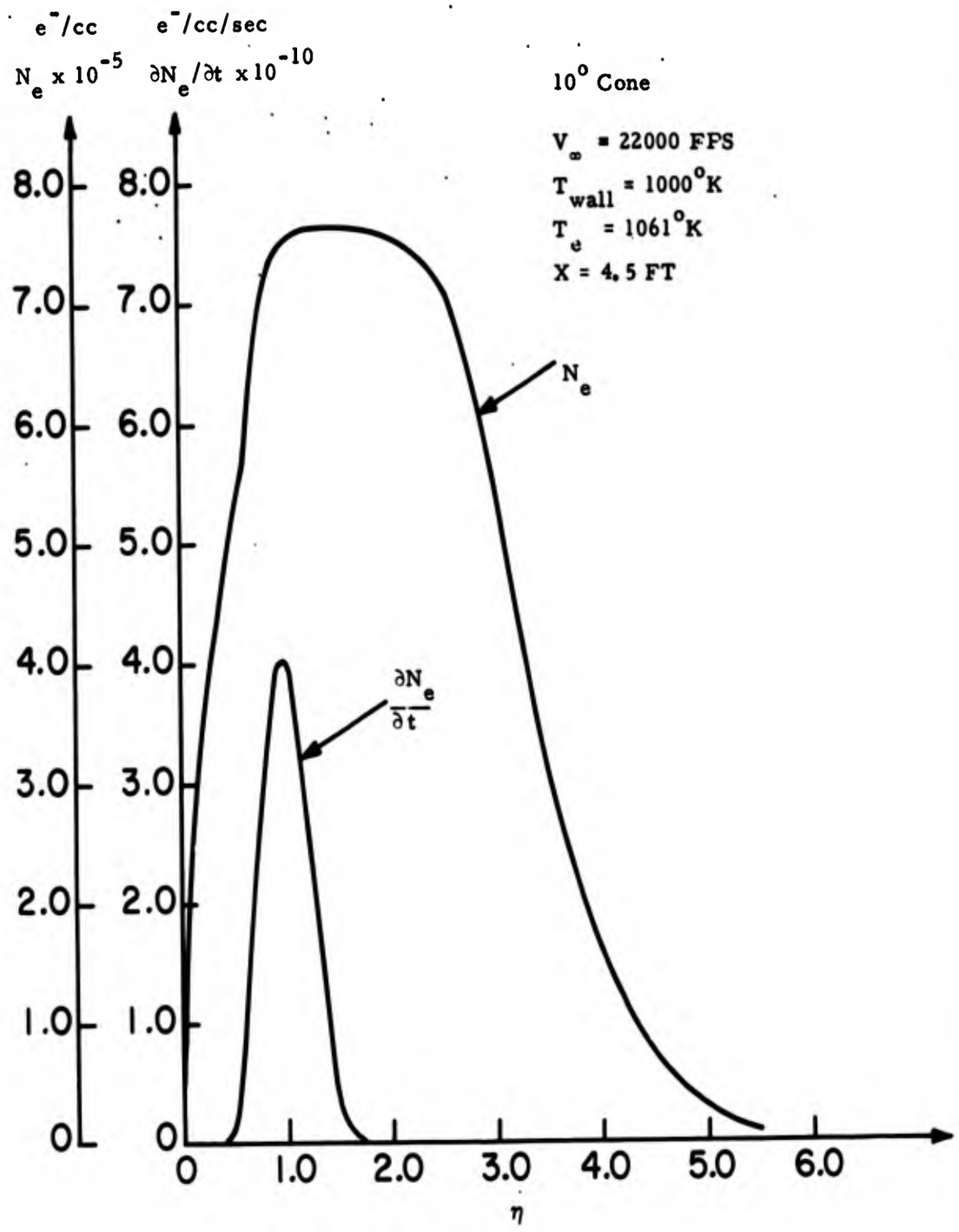

Figure 7. Electron Densities and Generation Rates in the Locally Similar Boundary Layer on a 10° Cone.

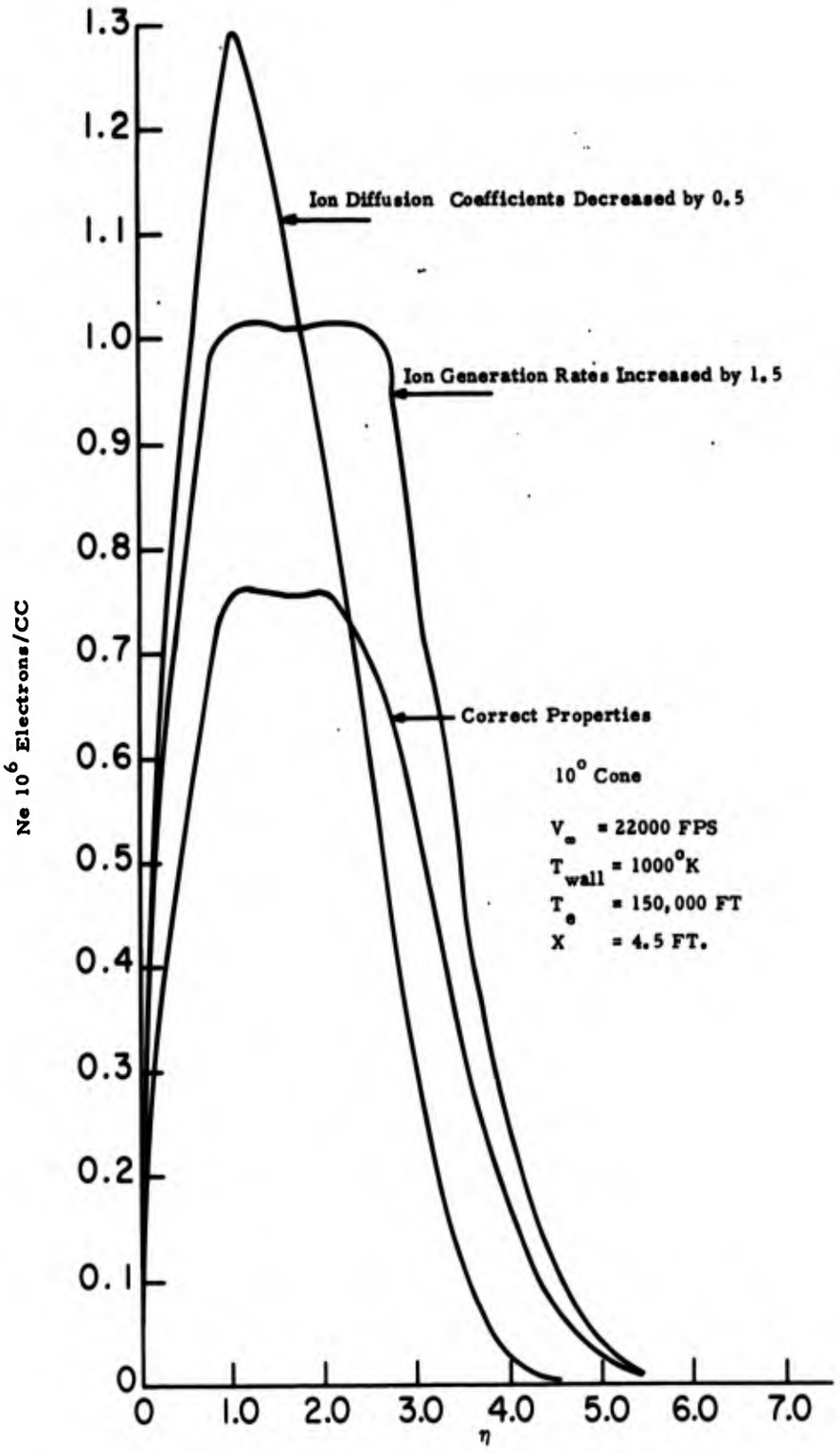

Figure 8. Effect of Ion Generation Rates and Ion Diffusivities on Electron Density in Locally Similar Boundary Layer on a 10° Cone

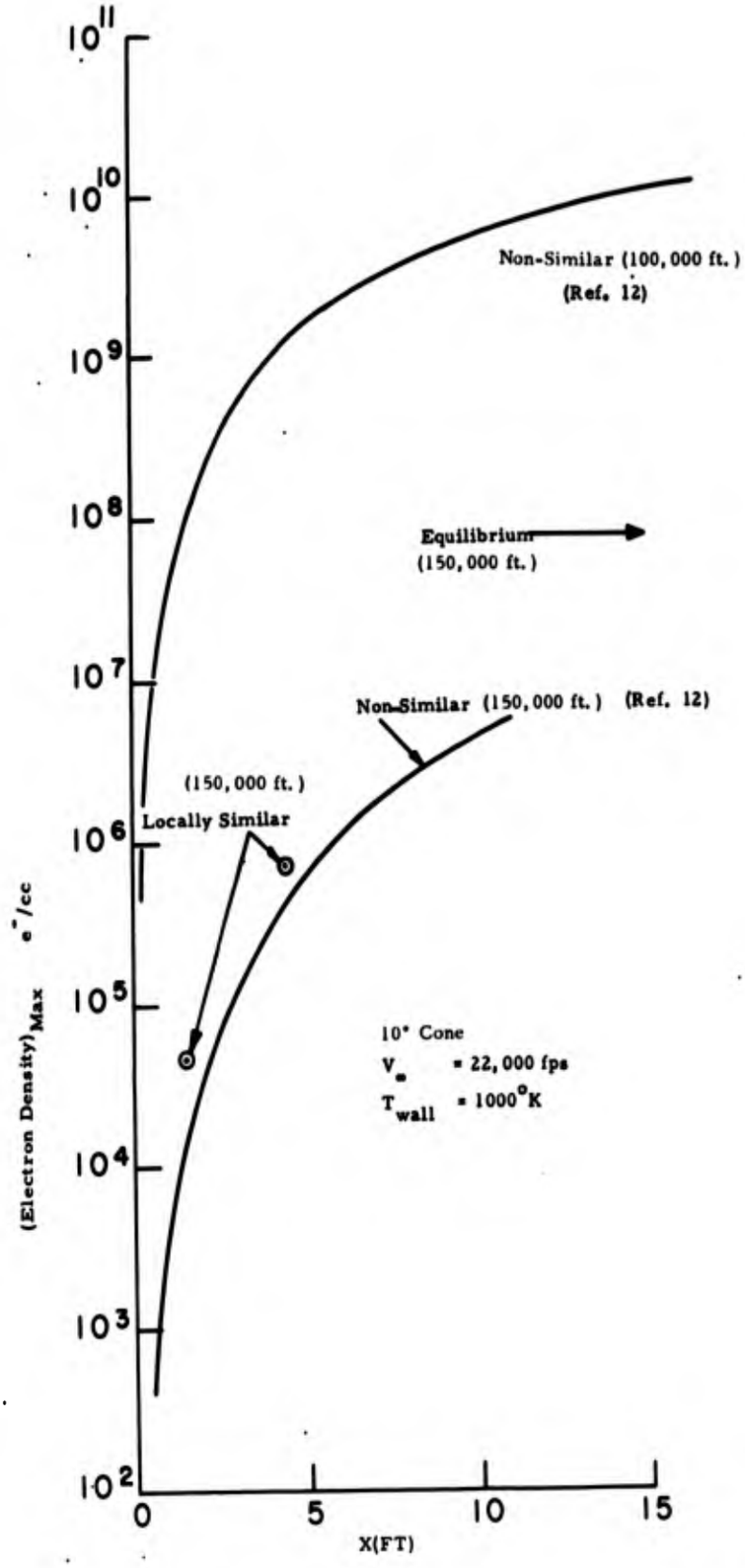

Figure 9. Maximum Electron Density in the Boundary Layer on a 10^{o} Cone

APPENDIX I

Chemical Properties

The species and chemical reactions were so chosen as to represent the ionizing process in pure air up to 10,000°K and at pressures corresponding to reentry conditions. The information is taken directly from Reference 5. Units of temperature are °K, units of concentration g moles/cc and units of the rate constants cm^3/g mole sec. or $cm^6/(g\ mole)^2$ sec. depending whether it is a two or three body reaction respectively. In order to convert these units into mass fractions used in the boundary layer calculations, the following conversion formulae are used:

$$\left[i\right] = \frac{\rho c_i}{m_i} \quad \frac{g\,moles}{cc} \qquad \text{(A1-1)}$$

$$\frac{d\left[i\right]}{dt} = \frac{w_i}{m_i} \quad \frac{g\ moles}{cc\ sec}$$

The reactions in Table AI are all endothermic in the forward (left to right) direction.

TABLE A1. REACTION RATE CONSTANTS

	Reaction	$k_{FORWARD}$	$k_{REVERSE}$	
1)	$O_2 + O_2 \rightleftharpoons O + O + O_2$	$2.3 \times 10^{19} T^{-1} e^{-59,400/T}$	$1.9 \times 10^{16} T^{-1/2}$	
2)	$O_2 + O \rightleftharpoons O + O + O$	$8.5 \times 10^{19} T^{-1} e^{-59,400/T}$	$7.1 \times 10^{16} T^{-1/2}$	
3)	$O_2 + M_3 \rightleftharpoons O + O + M_3$	$3.0 \times 10^{18} T^{-1} e^{-59,400/T}$	$2.5 \times 10^{15} T^{-1/2}$	$M_3 = N, N_2, NO, NO+$
4)	$O + N_2 \rightleftharpoons N + NO$	$6.8 \times 10^{13} e^{-37,750/T}$	1.5×10^{13}	
5)	$O + NO \rightleftharpoons N + O_2$	$4.3 \times 10^{7} T^{3/2} e^{-19,100/T}$	$1.8 \times 10^{8} T^{3/2} e^{-3020/T}$	
6)	$N + O \rightleftharpoons NO^+ + e^-$	$1.3 \times 10^{8} T\, e^{-31,900/T}$	$2 \times 10^{19} T^{-1}$	
7)	$N_2 + N_2 \rightleftharpoons N + N + N_2$	$3.8 \times 10^{19} T^{-1} e^{-113,200/T}$	$2 \times 10^{18} T^{-1}$	
8)	$N_2 + N \rightleftharpoons N + N + N$	$1.3 \times 10^{20} T^{-1} e^{-113,200/T}$	$7 \times 10^{18} T^{-1}$	
9)	$N_2 + M_9 \rightleftharpoons N + N + M_9$	$1.9 \times 10^{19} T^{-1} e^{-113,200/T}$	$1 \times 10^{18} T^{-1}$	$M_9 = O, O_2, NO, NO^+$
10)	$NO + M_{10} \rightleftharpoons N + O + M_{10}$	$2.4 \times 10^{17} T^{-1/2} e^{-75,500/T}$	$6 \times 10^{16} T^{-1/2}$	$M_{10} = O, O_2, N, N_2, NO^+$

Let the j-th reaction in this table be symbolically denoted by

$$j) \quad \sum_{i=1}^{n} \nu_{ji} \; i \rightleftharpoons \sum_{i=1}^{n} \nu'_{ji} \; i$$

where the unprimed and primed represent forward and backward reaction, ν_{ji} are the respective stoichiometric coefficients for the j-th reaction and the i-th species. The net production rate of the k-th species by the j-th reaction is then:

$$\left.\frac{d[k]}{dt}\right|_j = (\nu'_{jk} - \nu_{jk}) \left\{ k_j \prod_{i=1}^{n} [i]^{\nu_{ji}} - k'_j \prod_{i=1}^{n} [i]^{\nu'_{ji}} \right\} \qquad \text{(A1-2)}$$

The net production rate of the k-th species in the reacting mixture is obtained by summing equations (A1-2) over all the m reactions:

$$\frac{d[k]}{dt} = \sum_{j=1}^{m} (\nu'_{jk} - \nu_{jk}) \left\{ k_j \prod_{i=1}^{n} [i]^{\nu_{ji}} - k'_j \prod_{i=1}^{n} [i]^{\nu'_{ji}} \right\} \qquad \text{(A1-3)}$$

Equation (A1-3) together with (A1-1) relates the chemical mass generation rates w_i to the species mass fractions c_i at a specified thermodynamic state. The equilibrium composition $c_{j\,eq}(\rho, T)$ is obtained from a numerical solution of the system of non-linear algebraic equations:

$$w_i(\rho, T, c_{j\,eq}) = 0 \qquad \text{(A1-4)}$$

APPENDIX 2

Thermodynamic Properties

Enthalpies and specific heats of the species are determined by the use of partition functions:

$$h_i = \frac{R}{m_i}\left[T + T^2 \frac{\partial \ell n f_i}{\partial T}\right] \qquad \text{(A2-1)}$$

$$\frac{dh_j}{dT} = \frac{R}{m_i}\left[1 + 2T \frac{\partial \ell n f_i}{\partial T} + T^2 \frac{\partial^2 \ell n f_i}{\partial T^2}\right]$$

The units of the above expressions depend on a consistent choice of units for temperature, T, and the universal gas constant per mole, R. The expressions for the partition functions f_i and the constants involved therein are taken directly from Reference 4.:

$$f_i = \frac{a_i C_{T_i}}{o} e^{-\frac{E_{chem_i}}{\sigma T}} g_{1i}(f_{1i})^{b_{1i}} \qquad \text{(A2-2)}$$

where only one vibrational energy level was considered in the above expression, and the function f_{1i} is defined by:

$$f_{1i} = \frac{\sigma T}{hc} \frac{1}{B_i(1 - \frac{1}{2}\delta_i)(1 - e^{\nu_i})}\left\{1 + \frac{hc}{3\sigma T} B_i(1 - \frac{1}{2}\delta_i) + \right.$$

$$\left. + \frac{\sigma T}{hc} \frac{\dot{B}_i}{\omega_i^2 (1 - \frac{1}{2}\delta_i)} + \frac{\delta_i}{e^{\nu_i} - 1} + \frac{2X_i \nu_i}{(e^{\nu_i} - 1)^2}\right\} \qquad \text{(A2-3)}$$

Some symbols which appear exclusively in this Appendix in the above equations are defined as follows:

$$\nu_i \equiv \frac{ch}{\sigma T}(1 - 2X_i)$$

$$\kappa_i \equiv 6\frac{B_i}{w_i}\left[\left(\frac{\omega_i X_i}{B_i}\right)^{1/2} - 1\right] \qquad \text{(A2-4)}$$

$$C_{T_i} \equiv \left[\frac{2\pi\sigma T}{h^2 A_n} m_i\right]^{1/2}$$

Some general constants appearing in the above equations are:

$h = 6.624 \times 10^{-27}$ e·g sec

$A_n = 6.0228 \times 10^{23}$ molecules/mole

$\sigma = 1.38047 \times 10^{-16}$ ergs/^oK

$c = 2.99776 \times 10^{10}$ cm/sec

The table of constants associated with the individual species is as follows:

i	a_i	E_{chem_i} (ergs)	g_{1i}	b_{1i}	B_i (cm^{-1})	X_i	ω_i (cm^{-1})
N	1	1.562×10^{-11}	4	0	0	0	0
O	1	$.819 \times 10^{-11}$	3	0	0	0	0
N_2	1/2	0	1	1	1.990	.0060176	2358.07
O_2	1/2	0	3	1	1.446	.007639	1580.36
NO	1	$.161 \times 10^{-11}$	4	1	1.7046	.007337	1904.03
NO^+	1	1.644×10^{-11}	1	1	1.93	.006221	2170
e	2	0	0	0	0	0	0

Variations of h_i and $\frac{dh_i}{dT}$ vs. T are given in the tables below.

Table of $m_i h_i/R$ (^oK) vs. T (^oK)

Species	N	O	N_2	O_2	NO	NO+
T^oK 1000	59075	32164	3622	3772	14672	122061
2000	61575	34664	7786	8120	18944	126283
3000	64075	37164	12171	12607	23392	130701
4000	66575	39664	16638	17149	27904	135188
5000	69075	42164	21145	21726	32452	139713
6000	71575	44664	25679	26329	37027	144263
7000	74075	47164	30232	30955	41624	148832
8000	76575	49664	34803	35602	46239	153419
9000	79075	52164	39387	40269	50872	158021
10000	81575	54664	43985	44954	55521	162637

Table of $m_i \frac{dh_i}{dT}/R$ vs. T(^oK)

Species	N	O	N_2	O_2	NO	NO+
T^oK 1000	2.5	2.5	3.9284	4.1859	4.0746	4.0055
2000	2.5	2.5	4.3163	4.4445	4.3042	4.3576
3000	2.5	2.5	4.4365	4.5203	4.4873	4.4613
4000	2.5	2.5	4.4902	4.5610	4.5326	4.5090
5000	2.5	2.5	4.5220	4.5905	4.5626	4.5386
6000	2.5	2.5	4.5445	4.6151	4.5861	4.5605
7000	2.5	2.5	4.5624	4.6370	4.6063	4.5786
8000	2.5	2.5	4.5777	4.6572	4.6244	4.5945
9000	2.5	2.5	4.5915	4.6762	4.6413	4.6091
10000	2.5	2.5	4.6041	4.6943	4.6572	4.6227

APPENDIX 3

Transport Properties

Mixture viscosity and thermal conductivity were calculated by means of Wilke's semi-empirical formulae (Reference 6)

$$\mu = \sum_{i=1}^{n} \frac{X_i \mu_i}{\sum_{j=1}^{n} X_j \varphi_{ij}}$$

$$k = \sum_{i=1}^{n} \frac{X_i k_i}{\sum_{j=1}^{n} X_j \varphi_{ij}} \qquad \text{(A3-1)}$$

where

$$k_i = \mu_i \left[\frac{dh_i}{dT} + 1.25 \frac{R}{m_i} \right] \qquad \text{(A3-2)}$$

$$\varphi_{ij} = \frac{1}{\sqrt{8}} \left(1 + \frac{m_i}{m_j} \right)^{-1/2} \left[1 + \left(\frac{\mu_i}{\mu_j} \right)^{1/2} \left(\frac{m_j}{m_i} \right)^{1/4} \right]^2$$

and X_i are mole fractions which are related to mass fractions by the expression:

$$X_i = \frac{M}{m_i} c_i \qquad \text{(A3-3)}$$

The species viscosities μ_i were calculated from the collision integrals given in Reference 8:

$$\mu_i = 2.6693 \times 10^{-5} \frac{(m_i T)^{1/2}}{\Omega_i^{(2,2)}} \frac{g}{cm\ sec} \qquad \text{(A3-4)}$$

For the four species N, O, N_2, O_2 the collision integrals were as given in Reference 8 for the pure species, i.e., $\Omega^{(2,2)}_{N\text{-}N}$, etc.. For NO and NO^+ the following expression was used

$$\Omega^{(2,2)}_{NO\text{-}NO} = \Omega^{(2,2)}_{NO^+\,NO^+} = \frac{1}{4}\,\Omega^{(2,2)}_{N_2\text{-}N_2} + \frac{1}{4}\,\Omega^{(2,2)}_{O_2\text{-}O_2} + \frac{1}{2}\,\Omega^{(2,2)}_{O_2\text{-}N_2} \tag{A3-5}$$

The resulting viscosities were curve-fitted for the temperature range 1000 - 10,000°K as follows:

$$\mu_i = e^{\left[A_i(\ell n\, T)^2 + B_i(\ell n T) + c_i\right]} \frac{g}{cm\ sec} \tag{A3-6}$$

where T is in °K. The table of curve fit constants is as follows:

Table of Viscosity Curve Fit Constants

i	A_i	B_i	C_i
N	.0085863	.6463	-12.581
O	.020022	.43094	-11.246
N_2	.048349	-.022485	-9.9827
O_2	.038271	.021076	-9.5986
NO, NO^+	.042501	-.018874	-9.6197

The collision integrals tabulated in Reference 8 were also used to evaluate some of the binary diffusion coefficients by means of the expression:

$$\frac{p\mathcal{D}_{ij}}{p} = \frac{2.628 \times 10^{-3}\, T^{3/2}\, (m_i + m_j)^{1/2}}{p\,\Omega^{(1,1)}_{ij}\,(2\, m_i\, m_j)^{1/2}}\ cm^2/sec \tag{A3-7}$$

where p is in atmospheres and T in ^{o}K, Reference 8 tabulates $\Omega_{ij}^{(1,1)}$ for the following pairs: N_2 - O_2, N_2 - O, N_2 - N, O - O_2, O - N. The remaining neutral pairs were elevated by:

$$\Omega_{N-O_2}^{(1,1)} = \Omega_{N-NO}^{(1,1)} = \Omega_{N-N_2}^{(1,1)} \qquad \text{(A3-8)}$$

$$\Omega_{i-NO}^{(1,1)} = \frac{1}{2}\left[\Omega_{i-O_2}^{(1,1)} + \Omega_{i-N_2}^{(1,1)}\right] \text{ for } i = O,\ N_2,\ O_2$$

The binary diffusion coefficients for the NO^+ ions were obtained from Reference 7. All the $(p\mathcal{D}_{ij})$ - s were then curve-fitted by means of a formula identical to (A3-6). The following table of curve fit constants results:

Table of $\mathcal{D}_{ij}$ Curve Fit Constants (1 Atmosphere)

i-j	A	B	C
N - O	-.018485	2.1383	-12.786
N - N_2	.022067	1.4404	-10.151
N - O_2	.022067	1.4404	-10.151
N - NO	.022067	1.4404	-10.151
N - NO^+	-.10952	3.6620	-19.401
O - N_2	.022557	1.4361	-10,264
O - O_2	.014245	1.5070	-10.215
O - NO	.018046	1.4788	-10.277
O - NO^+	-.093476	3.3294	-17.689
N_2 - O_2	.03425	1.1209	-8.8703
N_2 - NO	.03826	1.1169	-9.0705
N_2 - NO^+	-.10764	3.6212	-19.634
O_2 - NO	.032626	1.1438	-8.9493
O_2 - NO^+	-.10772	3.6229	-19.628
NO - NO^+	-.10902	3.6877	-20.153
N - N	.0091080	1.6510	-10.567
O - O	.022861	1.4033	-9.9113
N_2 - N_2	.045160	1.0687	-9.1032
O_2 - O_2	.030690	1.1719	-9.0468
NO - NO	.0352	1.1318	-9.0109

GENERAL ELECTRIC

SPACE SCIENCES LABORATORY
MISSILE AND SPACE DIVISION

TECHNICAL INFORMATION SERIES

AUTHOR	SUBJECT CLASSIFICATION	NO.
M. Lenard	BOUNDARY LAYERS	R64SD14
		DATE: March, 1964
TITLE: CHEMICALLY REACTING BOUNDARY LAYERS		G. E. CLASS: I
		GOV. CLASS: None
REPRODUCIBLE COPY FILED AT MSD LIBRARY, DOCUMENTS LIBRARY UNIT, VALLEY FORGE SPACE TECHNOLOGY CENTER, KING OF PRUSSIA, PA.		NO. PAGES: 38

SUMMARY

Numerical calculations of the chemically reacting laminar air boundary layer equations are presented at several points along cone-shaped reentry bodies at several flight conditions and different wall temperatures. These results use a seven component, ten reaction model of air (N, O, N_2, O_2, NO, NO^+, e^-). Thermodynamic and transport properties are completely general and use the latest available information. The solutions are based on the assumption of local similarity. The resulting electron densities are noted.

KEY WORDS: Plasma sheath, Electron densities

BY CUTTING OUT THIS RECTANGLE AND FOLDING ON THE CENTER LINE, THE ABOVE INFORMATION CAN BE FITTED INTO A STANDARD CARD FILE

AUTHOR Michael Lenard

COUNTERSIGNED F. H. Clauser Fritz Trumpler for J.F.

UNCLASSIFIED